 SL, vol.4, no.1, pp.39-45, 2010

Simulation of Newtonian-Fluid Flows with C^2-Continuous Two-Node Integrated-RBF Elements

D.-A. An-Vo[1], N. Mai-Duy[1] and T. Tran-Cong[1]

Abstract: In this paper, the C^2-continuous control-volume method based on 2-node integrated radial basis function elements (IRBFEs) [CMES, vol.72, no.4, pp.299-334, 2011] are further developed for the simulation of incompressible viscous flows in two dimensions. Emphasis is placed on (i) the 2-node IRBFE discretisation of the stream function-vorticity formulation on Cartesian grids; and (ii) the development of a high order upwind scheme based on 2-node IRBFEs for the case of simulating convection-dominant flows. High levels of accuracy and efficiency of the present method are demonstrated by solving the lid-driven cavity problem.

Keywords: Integrated-radial-basis-function element, Cartesian grid, control volume, local approximation, upwind scheme.

1 Introduction

Cartesian-grid-based control-volume methods can be very economical owing to the fact that generating a grid and integrating the governing equations are low-cost. The approximations for the dependent variables and their spatial derivatives can be constructed globally on the whole grid or locally on small segments of the grid. An example of local approximation schemes is the standard control-volume (CV) method wherein the fluxes are estimated by a linear variation between two grid points, e.g. Patankar (1980). The use of two grid points allows for the consistency of the fluxes at CV faces - one of the four basic rules to guarantee a physically realistic solution (Patankar (1980)). With two-node-based local approximations, Cartesian-grid-based methods typically produce solutions which are continuous for the fields but not for their partial derivatives, i.e. C^0 continuity. The grid thus needs to be sufficiently fine to mitigate the effects of discontinuity of partial derivatives.

The Navier-Stokes (N-S) equations typically involve convection and diffusion terms. At high values of the Reynold number, the convection term is dominant and the nu-

[1] Computational Engineering and Science Research Centre, Faculty of Engineering and Surveying, The University of Southern Queensland, Toowoomba, QLD, 4350, Australia

merical simulation of the N-S equations becomes challenging. Various treatments for the convection term have been proposed in the literature. Those which take the influence of the upstream information of the flow into account, e.g. the upwind differencing and QUICK schemes, are known to provide a very stable solution. To maintain a high level of accuracy, an effective way is to employ high-order upwind schemes with the deffered-correction strategy.

Recently, a local high order approximant based on 2-node elements and integrated RBFs (IRBFs) for solving second-order elliptic problems in the CV framework has been proposed by An-Vo, Mai-Duy, and Tran-Cong (2011). It was shown that such elements lead to a C^2-continuous solution rather than the usual C^0-continuous solution. In this study, these C^2-continuous elements are extended to the simulation of viscous flows. In addition, high-order upwind treatments are incorporated in the proposed scheme to deal with convection-dominant flows.

The remainder of the paper is organised as follows. Brief reviews of the governing equations and integrated RBF elements are given in Section 2 and 3, respectively. Section 4 describes the proposed technique. The lid-driven cavity flow is presented in Section 5, followed by conclusions in Section 6.

2 Control-volume formulation

In this study, the method of modified dynamics or false transients is applied to obtain the structure of a steady flow. The N-S equations in terms of the stream function ψ and the vorticity ω are modified as

$$\frac{\partial^2 \psi}{\partial x^2} + \frac{\partial^2 \psi}{\partial y^2} + \omega = \frac{\partial \psi}{\partial t}, \tag{1}$$

$$\frac{\partial^2 \omega}{\partial x^2} + \frac{\partial^2 \omega}{\partial y^2} - Re\left(\frac{\partial \psi}{\partial y}\frac{\partial \omega}{\partial x} - \frac{\partial \psi}{\partial x}\frac{\partial \omega}{\partial y}\right) = \frac{\partial \omega}{\partial t}, \tag{2}$$

where $Re = UL/\nu$ is the Reynolds number, in which L is the characteristic length; U the characteristic speed of the flow; and ν the kinematic viscosity.

Integrating (1) and (2) over a CV of a grid point P, Ω_P, and applying the Green theorem to integrals leads to the following equations

$$\oint_{\Gamma_P}\left(\frac{\partial \psi}{\partial x}\mathrm{d}y - \frac{\partial \psi}{\partial y}\mathrm{d}x\right) + \int_{\Omega_P} \omega \mathrm{d}\Omega_P = \int_{\Omega_P} \frac{\partial \psi}{\partial t}\mathrm{d}\Omega_P, \tag{3}$$

$$\oint_{\Gamma_P}\left[\left(\frac{\partial \omega}{\partial x} - Re\omega\frac{\partial \psi}{\partial y}\right)\mathrm{d}y - \left(\frac{\partial \omega}{\partial y} + Re\omega\frac{\partial \psi}{\partial x}\right)\mathrm{d}x\right] = \int_{\Omega_P} \frac{\partial \omega}{\partial t}\mathrm{d}\Omega_P, \tag{4}$$

where Γ_P is the CV circumference. The governing differential equations (1) and (2) are thus transformed into a CV form (3)-(4).

3 Two-node IRBFEs

Consider an interior element, $\eta_1 \leq \eta \leq \eta_2$, and its two nodes are locally named as 1 and 2. Let $\phi(\eta)$ be a function to be approximated, and ϕ_1, $\partial\phi_1/\partial\eta$, ϕ_2 and $\partial\phi_2/\partial\eta$ be the values of ϕ and $\partial\phi/\partial\eta$ at the two nodes, respectively. The 2-node IRBFE scheme approximates $\phi(\eta)$ using two multiquadric-RBFs (MQs) whose centres are located at η_1 and η_2

$$\frac{\partial^2\phi}{\partial\eta^2}(\eta) = w_1\sqrt{(\eta-c_1)^2+a_1^2} + w_2\sqrt{(\eta-c_2)^2+a_2^2} = w_1 I_1^{(2)}(\eta) + w_2 I_2^{(2)}(\eta), \tag{5}$$

$$\frac{\partial\phi}{\partial\eta}(\eta) = w_1 I_1^{(1)}(\eta) + w_2 I_2^{(1)}(\eta) + C_1, \tag{6}$$

$$\phi(\eta) = w_1 I_1^{(0)}(\eta) + w_2 I_2^{(0)}(\eta) + C_1\eta + C_2, \tag{7}$$

where $I_i^{(2)}(\eta)$ denotes the MQ; c_i the MQ centre; a_i the MQ width; $I_i^{(1)}(\eta) = \int I_i^{(2)}(\eta)d\eta$; $I_i^{(0)}(\eta) = \int I_i^{(1)}(\eta)d\eta$ with $i = (1,2)$; and C_1 and C_2 the integration constants. Equations (7), (6) and (5) can be transformed into the physical space as

$$\phi(\eta) = \varphi_1(\eta)\phi_1 + \varphi_2(\eta)\phi_2 + \varphi_3(\eta)\frac{\partial\phi_1}{\partial\eta} + \varphi_4(\eta)\frac{\partial\phi_2}{\partial\eta}, \tag{8}$$

$$\frac{\partial\phi}{\partial\eta}(\eta) = \frac{\mathrm{d}\varphi_1(\eta)}{\mathrm{d}\eta}\phi_1 + \frac{\mathrm{d}\varphi_2(\eta)}{\mathrm{d}\eta}\phi_2 + \frac{\mathrm{d}\varphi_3(\eta)}{\mathrm{d}\eta}\frac{\partial\phi_1}{\partial\eta} + \frac{\mathrm{d}\varphi_4(\eta)}{\mathrm{d}\eta}\frac{\partial\phi_2}{\partial\eta}, \tag{9}$$

$$\frac{\partial^2\phi}{\partial\eta^2}(\eta) = \frac{\mathrm{d}^2\varphi_1(\eta)}{\mathrm{d}\eta^2}\phi_1 + \frac{\mathrm{d}^2\varphi_2(\eta)}{\mathrm{d}\eta^2}\phi_2 + \frac{\mathrm{d}^2\varphi_3(\eta)}{\mathrm{d}\eta^2}\frac{\partial\phi_1}{\partial\eta} + \frac{\mathrm{d}^2\varphi_4(\eta)}{\mathrm{d}\eta^2}\frac{\partial\phi_2}{\partial\eta}, \tag{10}$$

where $\{\varphi_i(\eta)\}_{i=1}^4$ is the set of basis functions in the physical space. Further details can be found in An-Vo, Mai-Duy, and Tran-Cong (2011).

4 Proposed method

Using the middle-point rule, equations (3) and (4) become

$$-\frac{A_P}{\Delta t}\psi_P + \left[\left(\frac{\partial\psi}{\partial x}\right)_e\Delta y - \left(\frac{\partial\psi}{\partial x}\right)_w\Delta y + \left(\frac{\partial\psi}{\partial y}\right)_n\Delta x - \left(\frac{\partial\psi}{\partial y}\right)_s\Delta x\right] = -A_P\left(\omega_P^0 + \frac{\psi_P^0}{\Delta t}\right), \tag{11}$$

$$-\frac{A_P}{\Delta t}\omega_P+\left[\left(\frac{\partial\omega}{\partial x}\right)_e\Delta y-\left(\frac{\partial\omega}{\partial x}\right)_w\Delta y+\left(\frac{\partial\omega}{\partial y}\right)_n\Delta x-\left(\frac{\partial\omega}{\partial y}\right)_s\Delta x\right]$$
$$+Re\left[-\left(\omega\frac{\partial\psi}{\partial y}\right)_e\Delta y+\left(\omega\frac{\partial\psi}{\partial y}\right)_w\Delta y+\left(\omega\frac{\partial\psi}{\partial x}\right)_n\Delta x-\left(\omega\frac{\partial\psi}{\partial x}\right)_s\Delta x\right]$$
$$=-\frac{A_P}{\Delta t}\omega_P^0, \quad (12)$$

where the superscript 0 represents the value obtained from the previous time level; the subscripts e,w,n and s the values of the property at the intersections of grid lines and the east, west, north and south faces of a CV; and A_P the area of Ω_P. Let E,W,N and S denote the east, west, north and south neighbouring nodes of P. One can form 4 two-node IRBFEs, namely WP,PE,SP and PN.

4.1 Diffusion approximations

The values of the flux at $x=x_e$ and $x=x_w$ are computed by means of the elements WP and PE, respectively, using (9)

$$\left(\frac{\partial\phi}{\partial x}\right)_e=\frac{\mathrm{d}\varphi_1(x_e)}{\mathrm{d}x}\phi_P+\frac{\mathrm{d}\varphi_2(x_e)}{\mathrm{d}x}\phi_E+\frac{\mathrm{d}\varphi_3(x_e)}{\mathrm{d}x}\frac{\partial\phi_P}{\partial x}+\frac{\mathrm{d}\varphi_4(x_e)}{\mathrm{d}x}\frac{\partial\phi_E}{\partial x}, \quad (13)$$

$$\left(\frac{\partial\phi}{\partial x}\right)_w=\frac{\mathrm{d}\varphi_1(x_w)}{\mathrm{d}x}\phi_W+\frac{\mathrm{d}\varphi_2(x_w)}{\mathrm{d}x}\phi_P+\frac{\mathrm{d}\varphi_3(x_w)}{\mathrm{d}x}\frac{\partial\phi_W}{\partial x}+\frac{\mathrm{d}\varphi_4(x_w)}{\mathrm{d}x}\frac{\partial\phi_P}{\partial x}, \quad (14)$$

where ϕ represents ψ and ω. Expressions for the flux at $y=y_n$ and $y=y_s$ are of similar forms.

4.2 Convection approximations

Let f be the intersection of the CV face and the grid line. The value of ω at point f is computed as

$$\omega_f=\omega_U+\Delta\omega_f, \quad (15)$$

where ω_U is the upstream value and $\Delta\omega_f$ the correction term that is a known value. $\Delta\omega_f$ is presently derived from the 2-node IRBFE approximation, i.e. (8). As an example, when $f\equiv w$ and $u_w>0$, one has

$$\omega_U=\omega_W, \quad (16)$$

$$\Delta\omega_f=(\varphi_1(x_w)-1)\omega_W^0+\varphi_2(x_w)\omega_P^0+\varphi_3(x_w)\frac{\partial\omega_W^0}{\partial x}+\varphi_4(x_w)\frac{\partial\omega_P^0}{\partial x}. \quad (17)$$

Velocity values in the convection term are simply estimated by a linear profile.

(a) $Re = 1000, 81 \times 81$ (b) $Re = 3200, 91 \times 91$

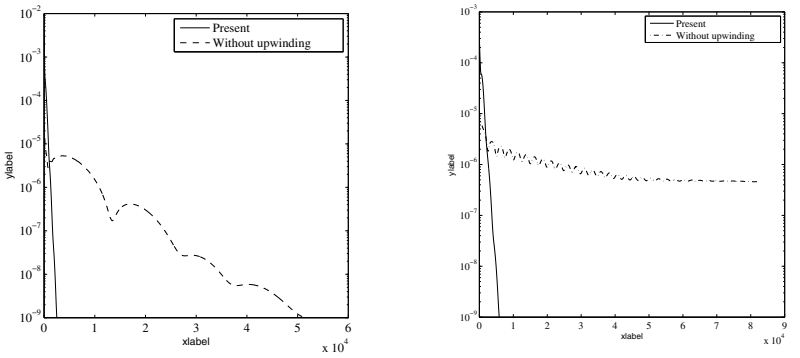

Figure 1: Convergence behaviours: present method using time steps of 3×10^{-4} in (a) and 10^{-4} in (b) converges remarkably faster than the no-upwind version using time step of 7×10^{-6} and 8×10^{-7}, respectively. It is noted that the latter diverges for time steps greater than 7×10^{-6} and 8×10^{-7}. *CM* denotes the relative norm of the stream-function field between two successive time levels.

5 Lid-driven cavity flow

In this study, the MQ shape parameter a is simply chosen proportionally to the element length h by a factor β. A large value of β, i.e. $\beta = 15$, is used in present calculations. The cavity is taken to be a unit square, with the lid sliding from left to right at a unit velocity. Boundary values of the vorticity are obtained by applying (10) as

$$\begin{aligned}\omega_b &= -\frac{\partial^2 \psi_b}{\partial \eta^2} \\ &= -\left(\frac{\mathrm{d}^2 \varphi_1(\eta_b)}{\mathrm{d}\eta^2} \psi_b + \frac{\mathrm{d}^2 \varphi_2(\eta_b)}{\mathrm{d}\eta^2} \psi_g + \frac{\mathrm{d}^2 \varphi_3(\eta_b)}{\mathrm{d}\eta^2} \frac{\partial \psi_b}{\partial \eta} + \frac{\mathrm{d}^2 \varphi_4(\eta_b)}{\mathrm{d}\eta^2} \frac{\partial \psi_g}{\partial \eta} \right), \end{aligned} \quad (18)$$

where η represents x and y.

The convergence behaviours with respect to time are shown in Fig. 1. Results without the upwind treatment are also presented. It can be seen that solutions converge remarkably faster for those with upwind than those without upwind. Much larger time steps can be used for the former. Tab. 1 reveals that the present results are closer to the benchmark spectral solutions than the global 1D-IRBF-CVM.

Table 1: $Re = 1000$: percentage errors relative to the spectral benchmark results (Botella and Peyret (1998)) for the extreme values of the velocity profiles on the vertical centreline. Results of upwind central difference (UW-CD), central difference (CD-CD) and global 1D-IRBF-CVM are taken from Mai-Duy and Tran-Cong (2010).

	Error (%)			
Grid	UW-CD	CD-CD	1D-IRBF-CVM	IRBFE-CVM
			u_{min}	
31x31	46.10	29.19	11.86	7.11
41x41	38.17	18.13	6.50	4.42
51x51	32.92	12.11	4.09	2.93
61x61	29.12	8.63	2.80	2.06
71x71	26.21	6.46	2.03	1.52
81x81	23.88	5.02	1.54	1.16
91x91	21.95	4.01	1.19	0.91
101x101	20.33	3.28	0.96	0.74
111x111	18.94	2.73	0.78	0.61
121x121	17.74	2.31	0.65	0.51

6 Concluding remarks

We have extended our 2-node IRBFEs to the solution of the stream function-vorticity formulation governing fluid flows. Numerical results show that (i) much larger time steps can be used with the upwind version; and (ii) a high level of accuracy is achieved.

Acknowledgement: D.-A. An-Vo would like to thank USQ, FoES and CESRC for a PhD scholarship. This research was supported by the Australian Research Council.

References

An-Vo, D.-A.; Mai-Duy, N.; Tran-Cong, T. (2011): A C^2-continuous control-volume technique based on Cartesian grids and two-node integrated-RBF elements for second-order elliptic problems. *CMES: Computer Modeling in Engineering and Sciences*, vol. 72 (4), pp. 299–334.

Botella, O.; Peyret, R. (1998): Benchmark spectral results on the lid-driven cavity flow. *Computers & Fluids*, vol. 27, pp. 421–433.

Mai-Duy, N.; Tran-Cong, T. (2010): A high-order upwind control-volume method based on integrated RBFs for fluid-flow problems. *International Journal for Numerical Methods in Fluids*, vol. early view.

Patankar, S. (1980): *Numerical heat transfer and fluid flow*. Taylor & Francis.